Environmental Science
Water Research & Technology

PAPER

View Article Online
View Journal | View Issue

Cite this: *Environ. Sci.: Water Res. Technol.*, 2017, **3**, 744

Effect of multicomponent fouling during microfiltration of natural surface waters containing nC_{60} fullerene nanoparticles†

R. Floris, ‡[ab] G. Moser, [a] K. Nijmeijer§[b] and E. R. Cornelissen*[ac]

Received 5th February 2017,
Accepted 17th May 2017

DOI: 10.1039/c7ew00041c

rsc.li/es-water

To understand and mitigate the role of surface water composition and associated membrane fouling in the removal of nC_{60} nanoparticles by low-pressure membranes, experiments were carried out with microfiltration membranes using natural feed waters, mimicking separation in real industrial water treatment plants. The effects of water composition, the presence of nanoparticles, and membrane fouling were investigated with a dead-end bench-scale system operated under constant flux conditions including a hydraulic backwash cleaning procedure. nC_{60} nanoparticles can be efficiently removed by microfiltration and the removal efficiency is found to be independent of the water surface composition. However, the water composition controls the extent of fouling occurring during filtration. A synergistic effect on membrane fouling between nC_{60} and surface water constituents such as natural organic matter (NOM) and its fractions is observed: the synergistic effect resulted in a transmembrane pressure (TMP) increase always higher than the sum of the TMP increase due to the filtration of nC_{60} in ultrapure water and the TMP increase due to the surface water without nC_{60}.

Water impact

The potential release of engineered nanoparticles into aquatic environments raises concerns on the security of resources used for drinking water production. It can also pose challenges to water treatment facilities in terms of operational optimization and proper process control. This research focuses on how membrane processes in drinking water plants can remove engineered nanoparticles and how these nanoparticles affect membrane operation performances.

1. Introduction

Given the growth of the nanotechnology industry in the past 20 years[1–3] and the accompanying increase in the amount of engineered nanomaterials and nanoparticles (eNPs) that enter the environment,[4] environmental and human health reasons require the investigation and assessment of the behaviour and toxicity of these new potential pollutants in natural and engineered environments. Buckminsterfullerene (C_{60})[5] is one of the most widely used eNPs[3,6] due to its particular physical and chemical properties,[7] *i.e.* heat resistance, conductivity and electron-acceptor capability. This explains its widespread use in different applications, *e.g.* cosmetics,[8] biological and medical applications[9,10] and plastic solar cells.[11] C_{60} can form nano-sized colloidal aggregates in water (usually and here as well referred to as nC_{60})[12] and can therefore potentially end up in aquatic compartments when released into the environment.

The presence of nC_{60} in aquatic environments[13] and consequently in sources for drinking water production[4] poses several challenges. Firstly, nC_{60} has been found toxic to several organisms (bacteria, fish and human cell lines[14–17]) and can function as a carrier for other pollutants such as adsorbed hydrophobic organic contaminants or heavy metals.[18–25] Therefore, its removal is mandatory for safe drinking water production. Secondly, nC_{60} will interact with water treatment systems affecting their performance, for instance causing fouling in microfiltration processes.[26,27] Both the removal of eNPs using microfiltration membranes and

[a] *KWR Watercycle Research Institute, PO Box 1072, 3430 BB Nieuwegein, The Netherlands. E-mail: emile.cornelissen@kwrwater.nl*
[b] *Membrane Science & Technology, Mesa+ Institute for Nanotechnology, University of Twente, PO Box 217, Enschede 7500 AE, The Netherlands*
[c] *Singapore Membrane Technology Centre, Nanyang Environment and Water Research Institute, Nanyang Technological University, Singapore 639798, Singapore*

† Electronic supplementary information (ESI) available. See DOI: 10.1039/c7ew00041c

‡ Current address: PWNT, Dijkweg 1, 1619 HA Andijk, The Netherlands.
§ Current address: Membrane Materials and Processes, Eindhoven University of Technology, PO Box 513, 5600 MB Eindhoven, The Netherlands.

the fouling of microfiltration membranes when filtering these eNPs are governed by complex interactions between the membrane and the eNPs, which is made even more complex due to the additional contribution of the natural background of water constituents. Particularly, natural organic matter (NOM, a complex mixture composed of different organic materials[28]) and divalent cations such as calcium and magnesium play a critical role in both eNP stability[29] and membrane fouling.[30–32]

Investigations into the effects of NOM on the aggregation of nC_{60} indicate that the presence of NOM results in diminished aggregation of eNPs, thus increasing their colloidal stability[33,34] by adsorption onto NOM leading to a more negatively charged surface.[35] NOM with a high average molar mass, low polarity and hydrophobic chains showed a good interaction with nC_{60} and increased the stability of nC_{60}.[36] High-molecular weight fractions of NOM such as large humic-like materials have been identified as key components for stabilizing nC_{60} in monovalent electrolyte solutions.[34,37] Electrostatic repulsion among nC_{60} was found positively correlated with the concentration of humic acid in solution.[38] The stabilization effect of NOM on nC_{60} might be achieved also through the reduced surface hydrophobicity.[39] Whilst humic substances tend to decrease aggregation and deposition of nC_{60}, the presence of multivalent cations induces aggregation[35] because of electrical double layer compression.[40] The presence of positively charged ions in water screens the negative surface charge of nC_{60} resulting in a more favorable condition for nC_{60} aggregation. The aggregation behavior of nC_{60} in the presence of NaCl, $MgCl_2$ and $CaCl_2$ was found to be consistent with the classic Derjaguin–Landau–Verwey–Overbeek (DLVO) theory of colloidal stability.[41] The simultaneous presence of humic acids and $CaCl_2$ in natural water resulted in an increased nC_{60} stability at low $CaCl_2$ concentrations, while enhanced aggregation occurred at high (>10 mM) $CaCl_2$ concentrations. The enhanced aggregation was attributed to intermolecular bridging of humic acid-coated nC_{60} by calcium.[29,37,38]

Not only does the composition of the water have an influence on the stability of nC_{60}, but the composition and the characteristics of the water also determine, to a large extent, membrane fouling.[42] Previous work has been carried out to understand the role of the amount, composition and properties of NOM and divalent cations in membrane fouling in drinking water treatment processes. NOM plays a significant role in fouling of microfiltration membranes even though it is retained only to a small extent.[43,44] The major contribution to fouling is attributed to the NOM fraction composed of biopolymers.[45] Meanwhile, the NOM fractions comprising humic and fulvic acids have only a minor contribution to microfiltration membrane fouling.[44] Shang *et al.* (2015)[46] found that, depending on the size of the membrane pores, the adsorption of NOM foulants can induce internal fouling. Based on experimental measurements, Yamamura *et al.* (2007)[47] proposed a two-step fouling model where hydrophobic low-molecular weight (humic-like) components are adsorbed first on the membrane surface, thereby narrowing the size of the membrane pores, followed by hydrophilic higher-molecular weight (carbohydrate-like) compounds that plug the narrowed pores of the membrane. Furthermore, the presence of calcium and its interactions with NOM play a major role in microfiltration fouling of surface waters.[48] Divalent cations reduce humic acid interchain repulsion resulting in the formation of a more densely packed fouling layer on the membrane surface.[31]

The studies mentioned above focused either on the interaction of divalent cations and NOM (fractions) or solely on membrane fouling or nC_{60} stability, but studies on the combined effect of multiple parameters, *i.e.* a comprehensive study combining the influence of divalent cations, NOM and its fractions on nC_{60} removal and membrane fouling in microfiltration of natural surface water, are still lacking, although essential to guarantee safe drinking water in the longer run. In the present study, we investigate the microfiltration behavior of nC_{60} dispersed in real surface water and focus on the elucidation of the role of NOM and divalent cations in (i) the removal of nC_{60} in semi dead-end hollow fiber microfiltration and (ii) membrane fouling during natural surface water microfiltration in the presence of nC_{60}. Filtration experiments with commercially available polymer membranes were conducted, including a regular backwash cleaning procedure with multiple cycles. The removal degree and removal mechanisms of fullerene nC_{60} were evaluated by analyzing transmembrane pressure (TMP) changes during filtration, evaluating the development of reversible and irreversible fouling and performing membrane autopsies with scanning electron microscopy observations.

2. Materials and methods

Reagents and chemicals

Fullerene-C_{60} (purity >99.5%) was obtained from Sigma Aldrich (Steinheim, Germany). Toluene was purchased from Mallinckrodt Baker B. V. (Deventer, The Netherlands).

Lewatit VPOC 1071 type (Lanxess, Germany) heterodisperse anion exchange gel-type resins were used for NOM removal. The anion exchange (AIEX) resins were based on a polyacrylamide backbone functionalized with quaternary amine (type I) groups. The average AIEX resin size was 0.55 mm and the resin density was 1.09 g ml^{-1}. Lewatit MonoPlus S 108 (Lanxess, Germany) monodisperse cation exchange resins were used for Ca^{2+}(aq) and Mg^{2+}(aq) removal. The cation exchange (CIEX) resins were based on a styrene–divinyl benzene copolymer. The average CIEX resin size was 0.65 mm and the resin density was 0.79 g ml^{-1}. Before use, both AIEX and CIEX resins were pre-rinsed and regenerated according to a procedure described elsewhere (Cornelissen *et al.*, 2010).[49] Briefly, 500 g of resin was rinsed for 12 h in 12.5 l of tap water. Afterwards, the resin was removed from the tap water and then mixed in 15 l of 10% w/w NaCl solution over 2 h for regeneration. Four different pre-treated water types were obtained after IEX treatment using the above described IEX resins employing the same surface water batch collected from the Lek Canal (Nieuwegein, The Netherlands) prior to the Amsterdam Water Supply Dunes (AWDs) uptake.

Preparation and characterization of nC_{60} dispersions

Stable aqueous nC_{60} suspensions were prepared using a solvent exchange/sonication procedure.[41] Briefly, 50 mg of C_{60} fullerene powder was added to 100 ml of toluene and the mixture was stirred for at least 12 h to achieve complete dissolution of the fullerenes. The C_{60} solution was added to 350 ml of ultrapure water (18.2 MΩ cm) in a 600 ml beaker. Toluene was evaporated in a sonication bath (Branson) at an energy intensity of 125 W. Ultrapure water was regularly added each hour to compensate for the volume loss due to toluene evaporation and to avoid fullerene deposition. The resulting colloidal dispersion was finally filtered through a 0.45 and a 0.22 μm cellulose acetate vacuum filter system (Corning Amsterdam, The Netherlands). This procedure was repeated 6 times resulting in nC_{60} stock concentrations of 15–20 mg l^{-1}. The obtained stock was diluted afterwards in the four different water types to reach a final concentration of 1 mg l^{-1}.

Characterization of the nC_{60} stock was performed with a set of different analytical techniques. The presence of colloidal dispersions was measured by UV–vis spectrophotometry. The nC_{60} UV/vis absorption spectrum of the stock displayed two typical peaks at 250 and 360 nm (not shown here), as was observed before (Jung, Kim, Kim & Kim, 2013).[50] Concentrations of nC_{60} were measured after liquid–liquid extraction with toluene[51] by using normal-phase liquid chromatography coupled to high-resolution mass spectrometry and UV spectrophotometry (LC-MS-UV). Due to the required concentration range, two approaches were used: (i) concentrations ranging from 0.1–128 μg l^{-1} were quantified by using the accurate molecular ion mass-to-charge ratio (m/z) of C_{60} (720.00055 m/z) and (ii) concentrations >128 μg l^{-1} were determined by UV spectrophotometry (at 335 nm).

The nC_{60} size distributions in the 4 different treated surface waters (directly after dosing nC_{60} in the surface water) were determined by dynamic light scattering (DLS). Measurements were performed with a Zetasizer Nano-ZS (Malvern Instruments, Worcestershire, UK). Samples were measured at 25 °C in triplicate. Zeta potential measurements were carried out using the same equipment to evaluate the surface charge and zeta potential of the nC_{60} (samples were measured 9 times per measuring point) in the 4 different treated surface waters (directly after dosing nC_{60} in the surface water). The average particle size of the nC_{60} in ultrapure water was determined by dynamic light scattering (146 nm), nanoparticle tracking analysis (134 nm) and analytical ultra-centrifugation (106 nm).[26] The zeta potential of nC_{60} in ultrapure water, measured in previous work, was −42.8 ± 1.33 mV.[26] This high zeta potential was also reported in several previous studies[52,53] and indicates high stability of the dispersion.

Preparation and characterization of water type backgrounds

To understand the role of the water quality parameters in the removal of nC_{60} by microfiltration, experiments were performed with nC_{60} dispersed in waters containing different amounts and compositions of NOM and in the presence or absence of divalent cations. The investigated water types were (i) pre-filtered surface water (PF), (ii) pre-filtered and anion exchange-treated surface water (AIEX), (iii) pre-filtered and cation exchange-treated surface water (CIEX) and (iv) pre-filtered and both anion and cation exchange-treated surface water (ACIEX). Filtration experiments involving nC_{60} dispersed in ultrapure water (Millipore, Bedford, MA) were also performed as a reference. Pre-filtered surface water was obtained by filtering the raw water subsequently through a 0.45 and a 0.22 μm cellulose acetate vacuum filter system (Corning Amsterdam, The Netherlands) to reduce turbidity and remove suspended solids present in the water. Anion and cation exchange-treated surface waters were obtained by stirring 25 l of such pre-filtered surface water with 500 g of resins for 24 h. The four water types were stored until use (maximum of 2 weeks) in the dark at 4 °C to minimize changes in the water composition before the experiments. The water compositions of the pre-filtered surface water and the anion, cation and anion/cation exchange-treated waters were determined by the laboratory of the water company Vitens (The Netherlands) with in-house methods VL-W-ACO1/02, VL-W-ME04, VL-T-AL35 and VL-W-00O2 according to NEN-EN-ISO/IEC 17025, NEN-EN-ISO 9001:2008, OHSAS 18001:2007 and ISO 14001:2004 standards.

Membrane and membrane characterization

Commercially available hollow fiber membranes made of a blend of polyethersulfone/polyvinylpyrrolidone were supplied by pentair X-Flow (Enschede, The Netherlands). According to the manufacturer and previous studies,[54,55] the membranes were moderately hydrophilic with pore diameters varying between 160 and 240 nm, having an average membrane pore size of 200 nm, with a highly asymmetric structure and selective layer several hundreds of nanometers in thickness on the inside of the fiber. The zeta potential of the inner surface of the membranes was −23 mV measured at pH 8 using a SurPASS electrokinetic analyser.[55]

Filtration set-up and procedure

All experiments were performed in constant flux and inside-out mode. Pure water flux (volumetric flow rate per unit area of the membrane) and nC_{60} filtration measurements were performed with a lab-scale pilot (Fig. 1a). A constant feed flow of 0.5 l h^{-1} was provided by a pulsation-free neMESYS syringe pump (Cetoni GmbH, Germany) connected to the feed vessel. A pressure sensor in the feed line measured the feed pressure every 5 seconds and an average transmembrane pressure (TMP) (n = 3) was calculated and logged every 15 seconds. A pressurized backwash vessel (3 bar) containing fresh ultra-pure water combined with a flow controller was connected to a permeate line for the backwash sequence. A backwash for 20 seconds occurred automatically every 20 min, which is a cleaning frequency relevant to membrane processes in drinking water treatment.[56] The total filtration duration was 2 hours including a series of 6 filtration cycles

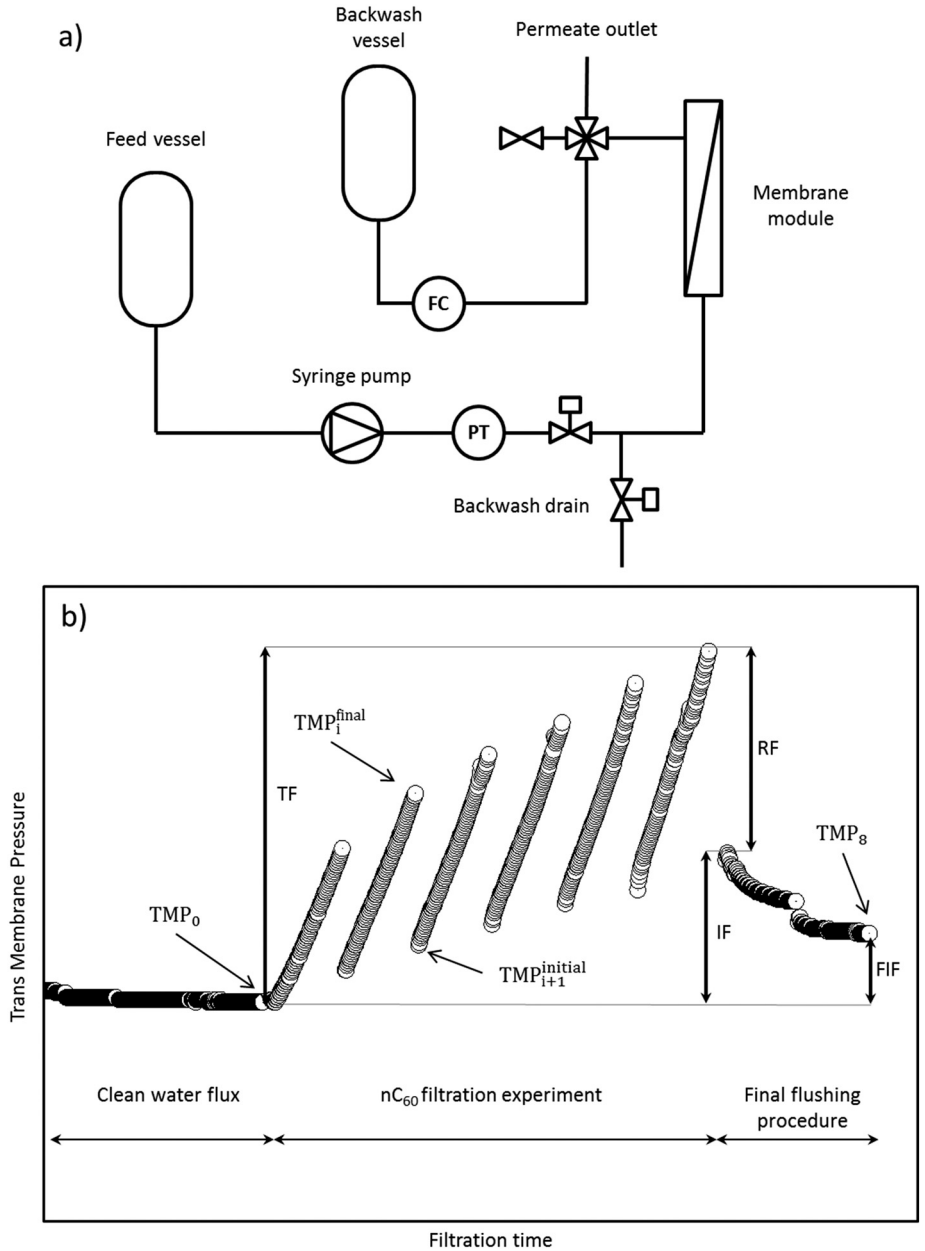

Fig. 1 a) Schematic representation of the lab-scale installation for constant flux filtration experiments; b) filtration protocol and fouling parameters as obtained from the TMP increase with time, where TF is the total fouling, RF is the reversible fouling, IF is the irreversible fouling, FIF is the final irreversible fouling after the final flushing procedure, TMP_i^{final} is the TMP at the end of filtration cycle *i* before the backwash cleaning procedure, TMP_{i+1}^{final} is the TMP at the beginning of filtration cycle *i* + 1 after the backwash cleaning procedure and TMP_0 is the TMP at the beginning of the experiment, immediately after the clean water flux measurement.

and 6 backwash sequences. All these experiments were performed at a constant temperature of 20 °C. Feed samples were collected before the experiments and permeate samples were collected during filtration cycle one, two, four and six to evaluate the nC_{60} removal at different filtration stages. After the last backwash, the membranes were flushed with ultrapure water to evaluate the membrane permeability recovery after nC_{60} filtration, from which the irreversible fouling contribution was calculated. This is an indirect indication of the amount of particles and other compounds that foul or adsorb onto the membrane and remain on the membrane after the flushing procedure. The flushing procedure consisted of 2 filtration cycles of ultrapure water at a constant feed flow (0.5 l h^{-1} for 20 min) followed by the backwash sequence (2 l h^{-1} for 20 s). A schematic representation of the filtration protocol is given in Fig. 1b.

Data handling

The removal efficiency (R [%]) for nC_{60} was evaluated as the nC_{60} rejection calculated from eqn (1):

$$R = \left(1 - \frac{C_p}{C_f}\right) \times 100 \quad (1)$$

where C_p is the permeate concentration and C_f is the feed concentration [mg l^{-1}].

To assess the type of fouling occurring during the filtration of nC_{60} using the low-pressure membranes, we analysed the evolution of measurable process parameters with time as follows:

Total Fouling (TF_i) at the generic cycle number i is the maximum increase in TMP during filtration, calculated according to eqn (2):

$$TF_i = TMP_i^{final} - TMP_0 \quad (2)$$

where TMP_i^{final} is the TMP at the end of filtration cycle i and before the backwash cleaning procedure and TMP_0 is the TMP at the beginning of the experiment, immediately after the clean water flux measurement.

Irreversible Fouling (IF) is the amount of foulant that cannot be removed by the backwash cleaning procedure only and accumulated in/on the membrane compromising the TMP. The IF at the generic cycle number i is calculated according eqn (3):

$$IF_i = TMP_{i+1}^{initial} - TMP_0 \quad (3)$$

In constant flux filtration, TMP increases linearly with time when an incompressible cake layer is formed.[57] In contrast, when the cake layer deposition is compressible, the pressure profile is concave-upward.[58] Additional analysis of the pressure profiles and the corresponding change of the slope (dTMP/dt) with time (or of the volume filtered) was performed to obtain more insight into the removal efficiency and the fouling mechanism.

3. Results and discussion

Water quality parameters

The water compositions of the pre-filtered surface water and anion, cation and anion/cation exchange-treated waters are given in Table 1.

All waters showed a low suspended solid content (<1 mg l^{-1}) and a low turbidity (~0.2 FTE) as a result of the pre-filtration treatment through the 0.45 and 0.22 μm filters. AIEX treatment reduced the NOM content measured as DOC by ~70%, which has been shown elsewhere to be mainly due to the removal of the humic substance fraction of the total NOM.[49] Based on Cornelissen *et al.*, we assumed that the remaining NOM fraction was mainly composed of neutrals, biopolymers and building blocks (*i.e.* hydrolysates of humic acids).[28,49] CIEX treatment almost completely removed the present divalent cations (>99% removal).

After both anion and cation exchange treatment, the waters showed an increase in conductivity. The increased value of water conductivity is due to the increased concentration of Na^+ and Cl^- released from the resins, as a consequence of the exchange process with NOM and Ca^{2+} and Mg^{2+}. This is also visible in Table 1, which shows higher concentrations of Na^+ and Cl^- in all treated waters compared to pre-filtered water (PF). The dissolved salt content can potentially affect the nC_{60} removal efficiency. However, it is also proven that destabilization of eNPs in water increases with increasing ion valence, due to higher compression of the eNP double layer.[24] In this study, we removed the amount of divalent cations (Ca^{2+} and Mg^{2+}) since these are the fractions of salinity in water that control the nC_{60} stability[52] and consequently its removal efficiency.

Table 1 Water quality parameters of the 4 water types

	Water types			
	PF	AIEX	CIEX	ACIEX
Turbidity (NTU)	0.2	0.2	0.2	0.2
Suspended solid [mg l^{-1}]	<1	<1	<1	<1
Conductivity (μS cm^{-1})	699	1560	1035	2210
pH	8.2	7.8	8.3	7.9
Zeta potential[b] (mV)	−10.1	−6.87	−7.93	−13.9
DOC (mg l^{-1})	2.9	0.7	3.2	0.8
Total hardness (mmol l^{-1})	2.4	2.3	<0.02	<0.02
Ca^{2+} (mg l^{-1})	76.0	74.2	<0.5[a]	<0.5[a]
Mg^{2+} (mg l^{-1})	11.8	11.1	<0.1[a]	<0.1[a]
K^+ (mg l^{-1})	3.9	3.8	0.3	0.4
Na^+ (mg l^{-1})	46.2	207.0	198	539.0
Cl^- (mg l^{-1})	86.0	380.0	160	550.0
NO_3^- (mg l^{-1})	13.7	2.6	—	4.0
SO_4^- (mg l^{-1})	55.0	<2	56	<2
HCO_3^- (mg l^{-1})	185.0	78.0	184	84.0

[a] Removal >99% from PF water. [b] Of the NOM and the colloidal particles naturally present in the water; *not measured.

nC_{60} size and zeta potential

The zeta potential and the average particle size of the nC_{60} dispersed in the 4 different treated surface waters are reported in Fig. 2.

When dispersed in natural water, nC_{60} is subject to stabilization effects of NOM and destabilization effects of cations present in the water. Dispersed particles are destabilized when their electrostatic surface charge is neutralized by positively charged ions.[59] On the other hand, the stability will increase as a result of the additional negative charge imparted by NOM adsorbed onto the nC_{60}.[41,60] The resultant impact of these two competitive effects can be analysed by zeta potential measurements. Colloids with a zeta potential more negative than −30 mV are considered to exhibit strong electrostatic repulsions and tend to remain dispersed, while a value of the zeta potential less negative than −30 mV makes them prone to aggregation and destabilization due to only weak electrostatic repulsions between the particles.[38,61]

From our zeta potential measurements, significant differences can be observed between water with Ca^{2+} and Mg^{2+} cations (PF and AIEX) and without Ca^{2+} and Mg^{2+} cations (CIEX

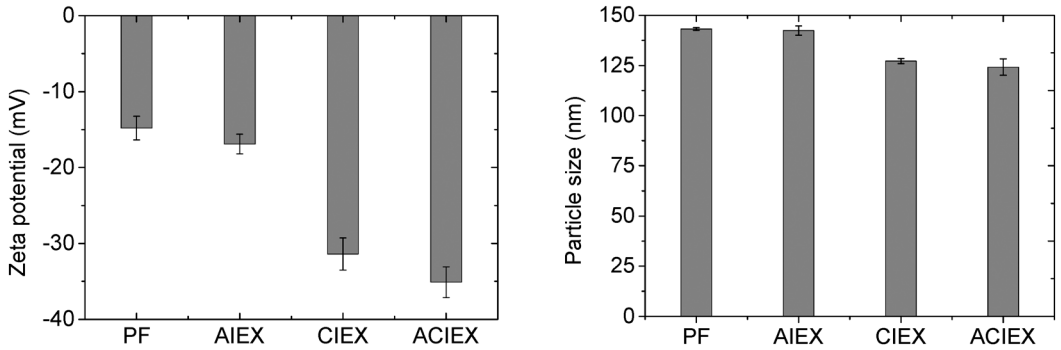

Fig. 2 Zeta potential and average particle size of nC_{60} dispersed in the 4 different treated surface waters (25 °C and pH 8 ± 0.2).

and ACIEX). Without these cations in the water, the value of the zeta potential is slightly higher than −30 mV (CIEX: −31.4 ± 2.13 mV and ACIEX: −35.1 ± 2.01 mV). Therefore, these two dispersions can most probably be considered stable. However, in apparent contradiction with previous studies, the change in zeta potential due to removal of NOM fractions was not observed most likely because of the different water background. Previous studies reported zeta potential values in synthetic water while here we used real (pre-treated) surface water. Therefore, the results reported here can still be considered general in the context of real surface waters. In contrast, when Ca^{2+} and Mg^{2+} are present in the water, these ions screen the nC_{60} surface charge and the zeta potential measured is less than −30 mV (PF: −14.8 ± 1.56 mV and AIEX: −16.9 ± 1.31 mV). This results in incipient instability of the dispersions.[62] The nC_{60} particles show comparable sizes in both PF (143.2 ± 0.7 nm) and AIEX (142.2 ± 2.3 nm) treated water, which is also in agreement with the nC_{60} size reported in ultrapure water (146 ± 1.9 nm (ref. 26)). This suggests that, despite the potential instability due to charge screening by Ca^{2+} and Mg^{2+}, agglomeration of the particles did not happen before the filtration experiments. The particle sizes in the absence of divalent cations (CIEX and ACIEX) are slightly smaller and measure approximately 127 ± 1 nm and 124 ± 4 nm. In the absence of divalent cations (CIEX and ACIEX), the particle sizes are also smaller than the nC_{60} particle size in ultrapure water. The smaller size of nC_{60} treated surface water does not depend on the presence of negatively charged NOM since both CIEX and ACIEX water show comparable particle size. Therefore, we hypothesize that this decrease in particle size is related to the interaction of nC_{60} with the neutral and positively charged fractions of NOM. However, regardless of the origin of the smaller nC_{60} size in the absence of divalent cations (CIEX and ACIEX), the ratio of nC_{60} size to mean membrane pore size (0.7/0.6) does not change significantly for the 4 water types analysed in this work.

Filtration behaviour of nC_{60} in different water backgrounds

Fig. 3 shows the TMP increase during microfiltration of the 4 different water types with the addition of 1 mg l^{-1} nC_{60} (black symbols). In the graphs, the TMP increases during microfiltration of (i) (treated) surface water without nC_{60} (PF, CIEX, AIEX or ACIEX) (dark grey) and (ii) a 1 mg l^{-1} nC_{60} dispersion in ultrapure water (light grey symbols) are also reported as references. Reference filtration experiments involving nC_{60} in ultrapure water and the 4 different water backgrounds without nC_{60} were performed to determine synergistic effects due to interactions between the water constituents and nC_{60}.

Filtration of 1 mg l^{-1} nC_{60} dispersed in ultrapure water resulted in a moderate TMP increase of 0.027 mbar over 6 filtration cycles (Fig. 3, light grey symbols). The TMP increase with time is due to pore blocking and cake layer deposition of the nC_{60} on the membrane surface.[26] The TMP increase is only partially reduced by the backwash procedure with an irreversible fouling contribution of about 57% of the total fouling in the case of nC_{60} in ultrapure water.

Filtration of 1 mg l^{-1} nC_{60} dispersed in surface water resulted in different TMP increases and fouling behaviors depending on the NOM fraction and the amount of Ca^{2+} and Mg^{2+} in the surface water used as a background (Fig. 3, black circles). Filtration of nC_{60} in waters containing the complete NOM fraction (PF and CIEX-treated waters) results in the highest increase of TMP (up to 1000 and 1200 mbar) over the 6 filtration cycles (Fig. 3a and b). The TMP increase is significantly reduced (in the range of 200–250 mbar) when the negatively charged NOM fractions are removed (AIEX- and ACIEX-treated waters, Fig. 3c and d), as a consequence of the lower amount of NOM (about 75% removal due to anion exchange treatment), which is thus responsible for the severe TMP increase.

The presence (PF and AIEX waters) or absence (CIEX and ACIEX waters) of Ca^{2+} and Mg^{2+} does not significantly impact the TMP increase within the 6 filtration cycles when the contribution of the NOM fraction is excluded. Consequently, the reduced stability of nC_{60} when bivalent cations are present (PF and AIEX) does not seem to affect the TMP increase during the filtration experiments.

Overall, despite differences in the amount of NOM and concentrations of Ca^{2+} and Mg^{2+} present in the different water backgrounds, in all cases, a strong synergistic effect between the nC_{60}, the cations and NOM during filtration of the different water types containing nC_{60} is observed. The TMP

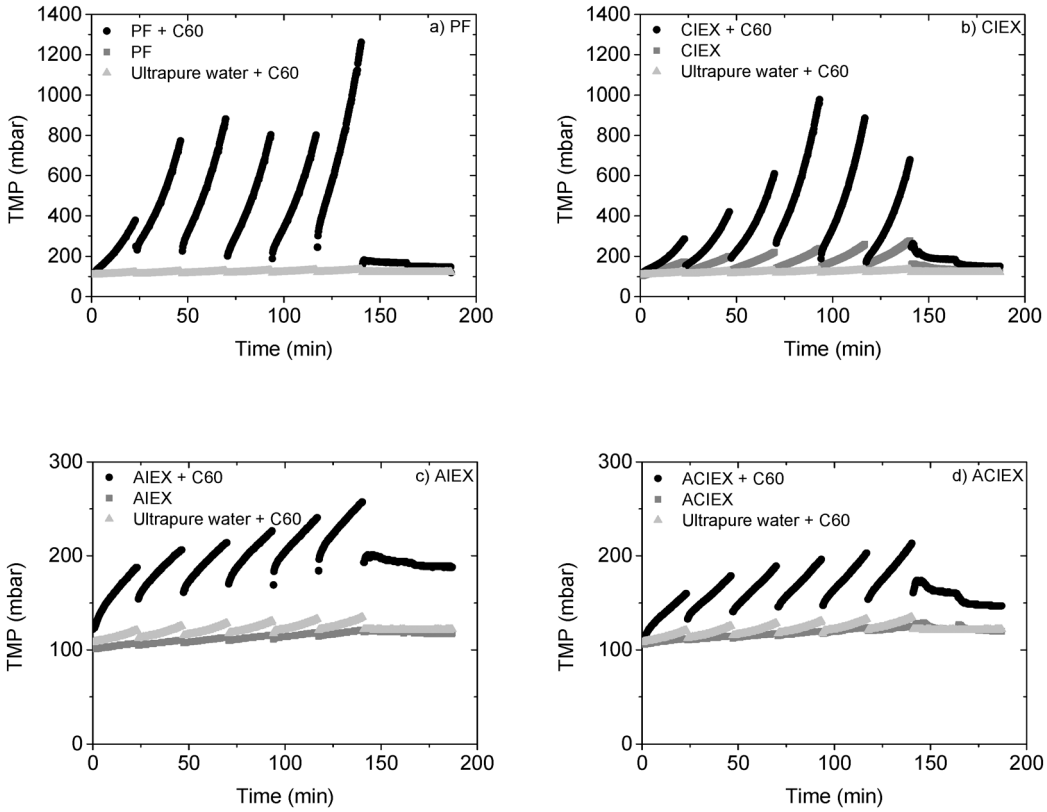

Fig. 3 TMP *versus* time for the filtration experiments involving nC_{60} in the four different water type backgrounds (black symbols): a) pre-filtered water, b) CIEX-treated water, c) AIEX-treated water and d) AIEX and CIEX-treated water. Corresponding experiments for the four different water types without nC_{60} (dark grey symbols) and for nC_{60} in ultrapure water (light grey symbols) are also shown as references (mind the different scales of the *Y*-axis).

increase is always higher than the sum of the TMP increase due to the filtration of nC_{60} in ultrapure water and the TMP increase due to the surface water without nC_{60}. This synergistic effect is especially dominant when the negatively charged NOM fraction is present in the water (Fig. 3a and b) and less dependent on the presence of divalent cations.

It is hypothesized that this synergetic effect is the result of different structural properties of the cake layer formed on top of the membrane surface, especially in the presence of negatively charged NOM. When only NOM is present in the water, the deposition layer formed on top of the membrane exhibits a certain cake porosity. During filtration of water simultaneously containing NOM and eNPs, the eNPs may fill the void spaces of the NOM deposited on the membrane surface, thus leading to a lower cake porosity and therefore a higher filtration resistance. In this scenario, it seems reasonable to assume a higher synergetic effect when all the NOM fractions are present in the water. Moreover, it was previously shown[63] that ultrafiltration of NOM (a mixture of humic acid and alginates (polysaccharides)) and inorganic particles (kaolinite with a particle size of 450 nm) resulted in a synergistic fouling effect due to particle stabilization by NOM and steric interferences between the two foulants. Although the particle size in our experiments is different and considerably smaller, similar effects in our filtration experiments are envisaged to take place.

To explain the synergistic effect, it can also be hypothesized that the interactions between nC_{60} and NOM can ultimately change the physical–chemical properties of the NOM and its fractions. Again, this will result in different structural properties of the cake layer formed on top of the membrane surface and different TMP increases. Both hypotheses need to be investigated more thoroughly and therefore future research in these directions is recommended.

Fig. 4 shows the total and the irreversible fouling (both expressed in TMP increase) over the six filtration cycles of nC_{60} dispersed in the 4 water backgrounds investigated. The total fouling and the irreversible fouling of the surface waters without nC_{60} are reported in the ESI† (Fig. S1).

The major fraction of the total fouling of waters containing the original NOM composition (PF and CIEX, Fig. 4a and b) is mostly reversible, which indicates that the backwashing procedure and the final flushing procedure (referred to as cycles number 7 and 8 in Fig. 4) enable the removal of the majority of the foulants accumulated on the membrane. The irreversible fouling is 5.8% for PF water and 24% for CIEX water at the end of cycle 6. The TMP is partially restored to the original value after the backwash cycles. This can be explained considering that a large part of the NOM (2.1 mg l^{-1} DOC, Table 1) in PF and CIEX water is composed of negatively charged humic acid, which forms a cake layer

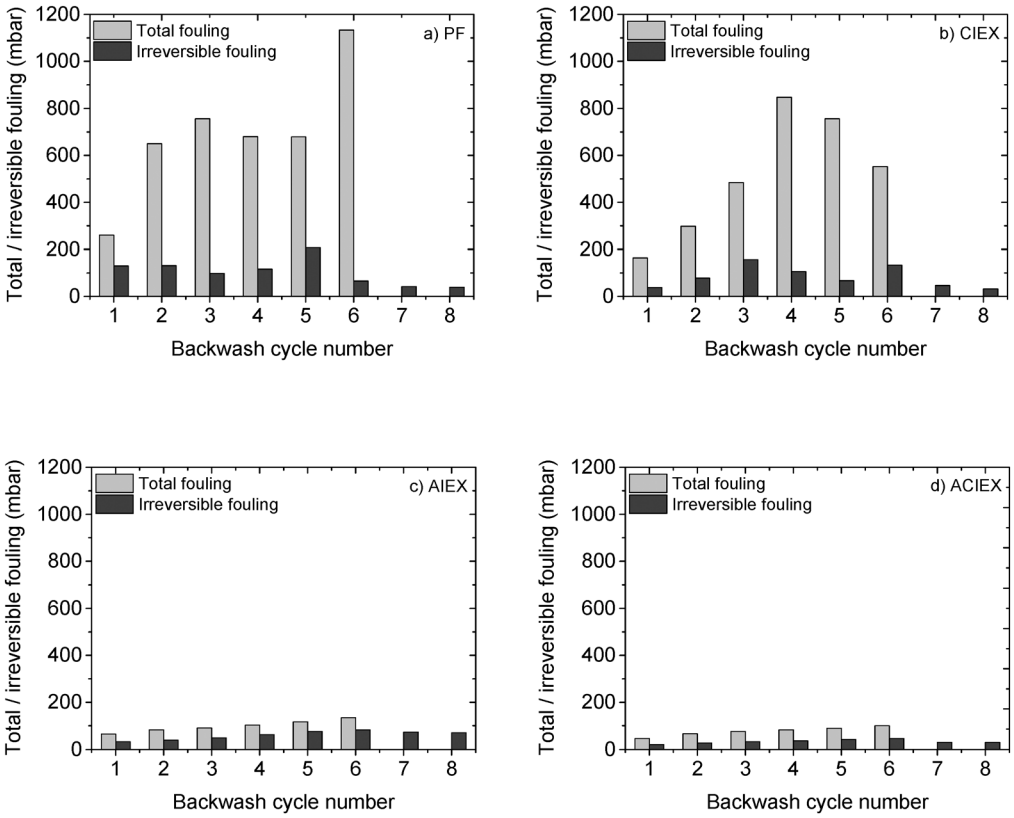

Fig. 4 Total fouling and irreversible fouling (expressed as pressure increase) *versus* the backwash cycle number for the various nC_{60} filtration experiments (cycles 1–6) on the four different water type backgrounds: a) pre-filtered water, b) CIEX-treated water, c) AIEX-treated water and d) ACIEX-treated water. Irreversible fouling after the final flushing procedure is also reported and referred to as cycles 7 and 8.

on the microfiltration membrane surface[64] that is apparently easily removed by the backwash procedure using ultrapure water.[65]

Nevertheless, when the cations are removed (CIEX), the remaining irreversible fouling at the end of the filtration experiment (after backwash cycle 6) is higher (24%) than that for PF water. This might be caused by the slightly smaller size of nC_{60} in CIEX-treated water (Fig. 2, CIEX), resulting in a more compact cake layer that is more difficult to remove. The evolution of irreversible fouling was not monotonic and this can be the result of different backwash efficiencies cycle by cycle. In addition, the slightly smaller size of nC_{60} in CIEX-treated water can also increase the occurrence of pore blocking at the beginning of the filtration cycle. In both cases (PF and CIEX-treated waters), the fouling that is not removed by backwash cycle 6 is partially removed after the final flushing procedure (cycles number 7 and 8) for both PF and CIEX-treated waters. A possible explanation is that the ultrapure water used in cycles number 7 and 8 removes some of the divalent cations from the cake layer making the following backwash procedure more effective in removing the cake layer.[66] This is also visible in the TMP increase (Fig. 3a and b) that can then be reduced to its original level.

Removing the negatively charged fraction of NOM (AIEX- and ACIEX-treated waters, Fig. 4c and d) results in a significant reduction of the total fouling. However, the results in Fig. 4 show that the total fouling that does occur is more persistent toward the backwash procedure (compared to PF and CIEX-treated waters). The irreversible fouling is about 62% (AIEX) and 48% (ACIEX) of the total fouling, and both the backwashing procedure during filtration and the final flushing procedure at the end of the nC_{60} filtration experiments are less effective and not sufficient to remove the foulants accumulated on the membrane. Particularly, when Ca^{2+} and Mg^{2+} are present in the water (AIEX-treated water, Fig. 4c), the irreversible fouling formed in the presence of these ions is more persistent. This can be attributed to enhancement of the irreversible fouling by divalent cation complexation and bridging with NOM.[32] Moreover, Ca^{2+} and Mg^{2+} can assist the formation of complexes (i) between NOM and nC_{60} and (ii) among nC_{60}, ultimately resulting in a more resilient cake layer.[33,41] This is indicated by a lower TMP decrease after flushing for the AIEX water compared to the ACIEX water (Fig. 4c and d).

Removal and fouling mechanism

In all cases, the observed nC_{60} removal efficiency was very high (99.99%) during all the filtration experiments (see Table S1, ESI†). This is in accordance with the removal efficiencies previously obtained for the filtration of nC_{60} dispersed in ultrapure water.[26] The removal efficiency was found to be

independent of the type of water (Table S1†), although the pressure profiles reported in Fig. 3 suggest different fouling behaviours for the differently treated waters. Although the average nC_{60} size in surface water is slightly smaller than the size when dispersed in ultrapure water,[26] the ratio of nC_{60} size and mean membrane pore size is still comparable. We showed previously[26,55] that the microfiltration membrane used has an asymmetric pore size distribution with smaller pores on the inside of the fiber. When it is dispersed in ultrapure water, this resulted in complete removal of nC_{60} by a combination of size exclusion and pore blockage. Moreover, if nC_{60} does not permeate during the first filtration cycle, it is unlikely that permeation will happen in the following cycles as fouling and pore blocking become even more severe during the course of the filtration process. This explains the high removal efficiency during all the cycles of the filtration experiments.

Fig. 5 reports the development of the slopes (dTMP/dt) of the pressure profiles with time for the 4 different water dispersions and for the first filtration cycle, which is representative of the slopes during all cycles. Slope trends for the remaining cycles 2–6 show similar behaviour to the first one and are reported in the ESI† (Fig. S2). Analysis of the pressure profiles and the change of the slope as a function of time (dTMP/dt, or of the volume filtered dTMP/dV) can provide insight into the removal and fouling mechanisms occurring.[58]

In constant flux filtration, when the cake layer is incompressible, the TMP increases linearly (with constant dTMP/dt) with time.[57] In contrast, when the deposited cake layer is compressible, the pressure profile is convex, so dTMP/dt is not constant but increases with time.[58]

For all investigated waters, as presented in Fig. 5, a first transition zone (from 0 to ~4 min) can be identified. In this transition zone, the slope, dTMP/dt, first increases and afterwards decreases again. In this transition zone, most likely pore blocking occurs, as was observed in other studies.[55,67] After this transition zone, different behaviours are visible for the different water types. For AIEX- and ACIEX-treated waters, the slope dTMP/dt stabilizes to a constant value (~2 mbar min^{-1}), which indicates that the TMP increase is linearly related to the filtration time, and thus an incompressible cake layer is formed on the membrane surface.[58] In contrast, for water containing all NOM fractions (CIEX and PF waters), after the first initial 4 minutes, the slope, dTMP/dt, linearly increases with time, which means that the cake layer formed on the membrane surface is compressible. During fouling, a compressible cake layer is formed, ultimately increasing the hydraulic resistance, and thus the TMP increase, during constant flux filtration.[57]

It can be hypothesized that the occurrence of a compressible or incompressible cake layer depends on the presence and amount of organic foulants present in the 4 water types:

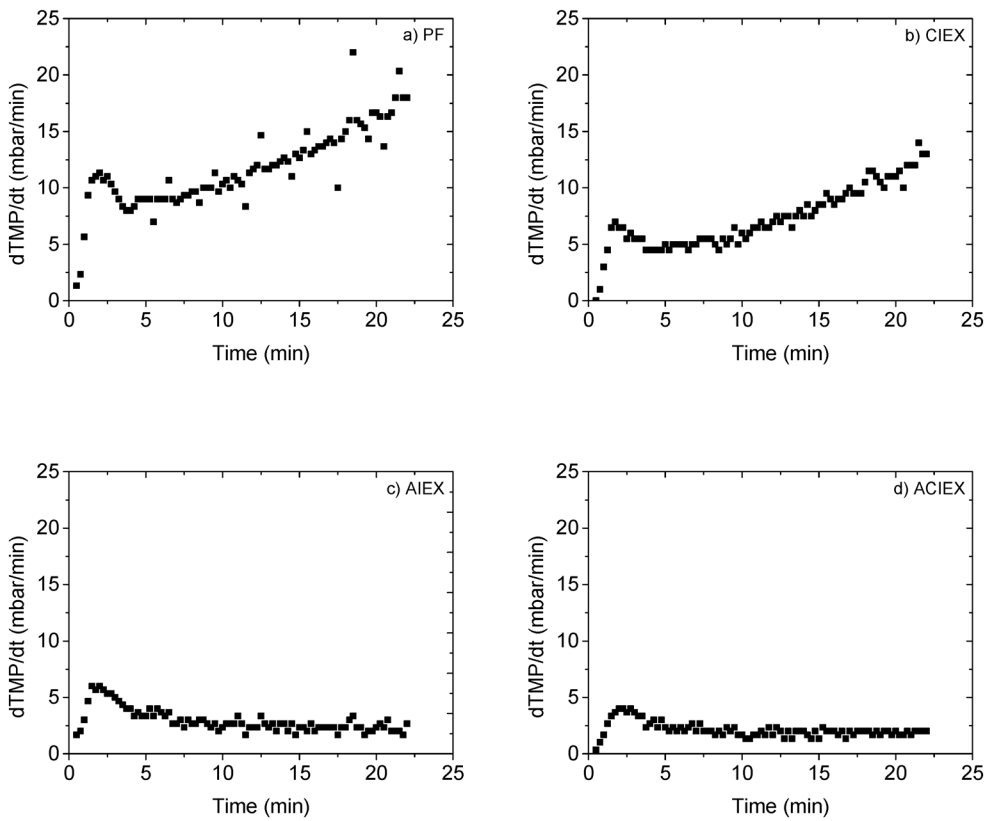

Fig. 5 Change of dTMP/dt with time for the 4 different water types: a) PF water; b) CIEX-treated water; c) AIEX-treated water; d) ACIEX-treated water.

the literature shows that, during dead-end filtration, the TMP can compress the cake layer and reduce its thickness.[68] However, this is only possible when a certain critical amount of foulants is deposited on the membrane. Below this critical value, the structure of the cake layer remains the same, independent of the TMP. Above this limit, the cake layer becomes compressible and its thickness and porosity decrease with increasing TMP. This scenario seems also applicable to our work for the 4 different water type backgrounds without eNPs (ESI†). For ACIEX- and AIEX-treated waters, the slope dTMP/dt is constant over all cycles. In contrast, the behaviour of the slope with time for waters containing NOM (PF and CIEX-treated waters) indicates the occurrence of two different stages during the formation of the cake layer and its growth: first, the formation of an incompressible cake layer (until cycle 2), and subsequently the transformation of this layer into a compressible layer (after cycle 3). Therefore, it is possible that waters containing both NOM and nC_{60} already at the first filtration cycle have a total load of foulants higher than the critical value, which makes the cake layer compressible. Nonetheless, the occurrence of synergistic fouling effects of nC_{60}–NOM (fractions) cannot be excluded, due to particle stabilization by NOM or steric interferences between the two foulants.[63] Therefore, the high increase in TMP observed in Fig. 3a and b (PF and CIEX-treated waters) can be attributed to (i) the large amount of organic foulants in the water (compared to AIEX- and ACIEX-treated waters (Fig. 3c and d)) and (ii) cake layer compressibility.

Assuming that pore blocking occurs only at the initial stage of the filtration cycle, as filtration proceeds, the increase of the filtration resistance with time can be related to the formation of a cake layer deposit,[55,67] as confirmed by the SEM photos of the internal membrane surfaces after the filtration experiments (Fig. 6). In all cases, a thick deposition layer (>150 nm) on the membrane surface can be observed (at the right side of the images), even after the final flushing procedure.

4. Conclusions

The removal of nC_{60} using microfiltration was investigated using pre-filtered natural surface water and pre-filtered natural surface water without multivalent cations and/or without the negatively charged part of NOM.

Microfiltration membranes are a solid barrier to remove nC_{60} from surface water during drinking water production and the removal efficiency is found to be >99.99% and independent of the surface water composition. However, a synergistic effect on membrane fouling between nC_{60} and surface water constituents such as NOM and its fractions is observed.

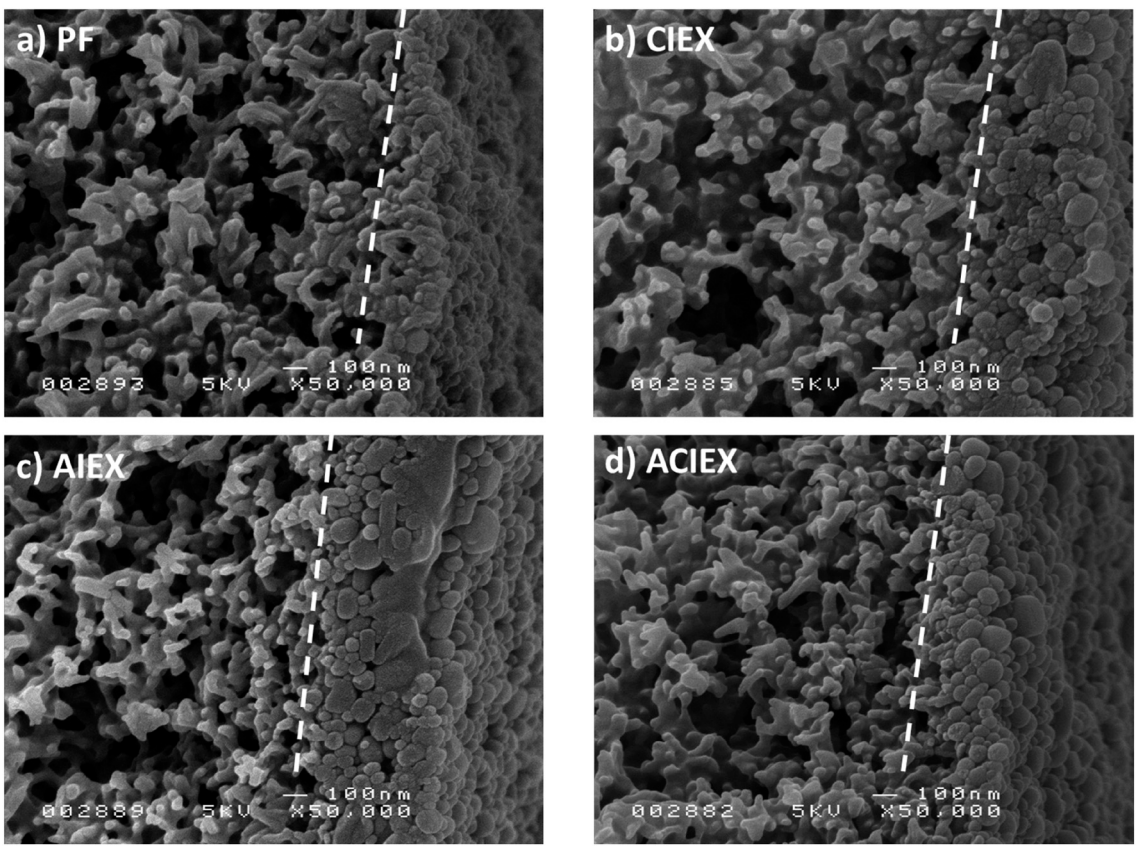

Fig. 6 SEM images of fouled membranes after 6 filtration and backwash cycles and a final flushing step: a) PF water; b) CIEX-treated water; c) AIEX-treated water; d) ACIEX-treated water.

Although Ca^{2+} and Mg^{2+} are dominant in controlling the stability of nC_{60} (*i.e.* particle size and particle zeta potential), the extent of fouling is dominated by the presence of NOM. The negatively charged NOM fractions lead to the formation of a compressible cake layer. Removing this fraction from the feed water results in the formation of an incompressible cake layer and a reduction of the TMP increase during filtration. Despite the removal of the negatively charged fraction of NOM, the presence of the divalent cations Ca^{2+} and Mg^{2+} enhances the formation of irreversible fouling, reducing the efficiency of backwash and final flushing procedures in restoring the initial TMP.

These results confirm the resilience of microfiltration in removing nC_{60} from water under relevant environmental conditions. The results provide insight into the effect of the constituents in natural water on the effectiveness of membrane filtration to retain nC_{60}, which is essential to guarantee safe drinking water in the longer run.

Acknowledgements

This research was sponsored by the Joint Research Programme of KWR Watercycle Research Institute for the Dutch Drinking Water Companies and supported by NanoNextNL, a micro- and nanotechnology consortium of the Government of the Netherlands and 130 partners. The authors would also like to acknowledge Herman Teunis (European Membrane Institute Twente) for the SEM analysis, Jens Potreck (pentair X-Flow) for providing the membranes, Ron Jong (Vitens) for the surface water analysis, Krzysztof Trzaskus (University of Twente) for the help in the nC_{60} and membrane characterization, and Erik Emke and Margo van der Kooi (KWR Watercycle Research Institute) for the C_{60} concentration analysis. The authors would specially like to thank Harry van Wegen and Sydney Meijering for the assistance with the lab set-up.

References

1 T. M. Benn, P. Westerhoff and P. Herckes, Detection of fullerenes (C60 and C70) in commercial cosmetics, *Environ. Pollut.*, 2011, **159**(5), 1334–1342.
2 H. Murayama, S. Tomonoh, J. Alford and M. E. Karpuk, Fullerene production in tons and more: From science to industry, *Fullerenes, Nanotubes, Carbon Nanostruct.*, 2004, **12**(1–2), 1–9.
3 *Perspective of Fullerene Nanotechnology*, ed. E. Osawa, Springer, Berlin, Germany, 2002.
4 F. Gottschalk, T. Sun and B. Nowack, Environmental concentrations of engineered nanomaterials: review of modeling and analytical studies, *Environ. Pollut.*, 2013, **181**, 287–300.
5 H. W. Kroto, J. R. Heath, S. C. O'Brien, R. F. Curl and R. E. Smalley, C60: Buckminsterfullerene, *Nature*, 1985, **318**, 162.
6 J. R. Baena, M. Gallego, M. Valca and A. C. Division, Fullerenes in the analytical sciences, *TrAC, Trends Anal. Chem.*, 2002, **21**(3), 187–198.
7 D. Guldi and M. Prato, Excited-State Properties of C60 Fullerene Derivatives, *Acc. Chem. Res.*, 2000, **33**(10), 695–703.
8 M. S. Reisch, Innovation: Novel ingredients spread across in cosmetics, *Chem. Eng. News*, 2009, **87**, 12–13.
9 A. W. Jensen, S. R. Wilson and D. I. Schuster, Biological Applications of Fullerenes, *Bioorg. Med. Chem.*, 1996, **4**(6), 767–779.
10 R. Bakry, R. M. Vallant, M. Najam-ul-Haq, M. Rainer, Z. Szabo and C. W. Huck, *et al.* Medicinal applications of fullerenes, *Int. J. Nanomed.*, 2007, **2**, 639–649.
11 C. J. Brabec, N. S. Sariciftci and J. C. Hummelen, Plastic Solar Cells, *Adv. Funct. Mater.*, 2001, **11**(1), 15–26.
12 S. Deguchi, R. G. Alargova and K. Tsujii, Stable Dispersions of Fullerenes, C60 and C70, in Water. Preparation and Characterization, *Langmuir*, 2001, **17**, 6013–6017.
13 M. Farré, S. Pérez, K. Gajda-schrantz, V. Osorio, L. Kantiani and A. Ginebreda, *et al.* First determination of C60 and C70 fullerenes and N-methylfulleropyrrolidine C60 on the suspended material of wastewater effluents by liquid chromatography hybrid quadrupole linear ion trap tandem mass spectrometry, *J. Hydrol.*, 2010, **383**(1–2), 44–51.
14 S.-R. Chae, S. Wang, Z. Hendren, M. Wiesner, Y. Watanabe and C. Gunsch, Effects of fullerene nanoparticles on *Escherichia coli* K12 respiratory activity in aqueous suspension and potential use for membrane biofouling control, *J. Membr. Sci.*, 2009, **329**(1–2), 68–74.
15 D. Y. Lyon, L. K. Adams, J. C. Falkner and P. J. J. Alvarezt, Antibacterial activity of fullerene water suspensions: effects of preparation method and particle size, *Environ. Sci. Technol.*, 2006, **40**(14), 4360–4366.
16 C. M. Sayes, A. M. Gobin, K. D. Ausman, J. Mendez, J. L. West and V. L. Colvin, Nano-C60 cytotoxicity is due to lipid peroxidation, *Biomaterials*, 2005, **26**(36), 7587–7595.
17 M. Song, S. Yuan, J. Yin, X. Wang, Z. Meng and H. Wang, *et al.* Size-dependent toxicity of nano-C60 aggregates: more sensitive indication by apoptosis-related Bax translocation in cultured human cells, *Environ. Sci. Technol.*, 2012, **46**(6), 3457–3464.
18 B. Xie, Z. Xu, W. Guo and Q. Li, Impact of natural organic matter on the physicochemical properties of aqueous C60 nanoparticles, *Environ. Sci. Technol.*, 2008, **42**(8), 2853–2859.
19 T. Hofmann and F. von der Kammer, Estimating the relevance of engineered carbonaceous nanoparticle facilitated transport of hydrophobic organic contaminants in porous media, *Environ. Pollut.*, 2009, **157**(4), 1117–1126.
20 E. Navarro, A. Baun, R. Behra, N. B. Hartmann, J. Filser and A.-J. Miao, *et al.* Environmental behavior and ecotoxicity of engineered nanoparticles to algae, plants, and fungi, *Ecotoxicology*, 2008, **17**(5), 372–386.
21 V. Stone, B. Nowack, A. Baun, N. van den Brink, F. Von Der Kammer and M. Dusinska, *et al.* Nanomaterials for environmental studies: classification, reference material issues, and strategies for physico-chemical characterisation, *Sci. Total Environ.*, 2010, **408**(7), 1745–1754.

22 N. Musee, Nanowastes and the environment: Potential new waste management paradigm, *Environ. Int.*, 2011, **37**(1), 112–128.
23 K. Yang, L. Zhu and B. Xing, Adsorption of Polycyclic Aromatic Hydrocarbons by Carbon Nanomaterials, *Environ. Sci. Technol.*, 2006, **40**(6), 1855–1861.
24 L. Zhang, Q. Zhao, S. Wang, H. Mashayekhi, X. Li and B. Xing, Influence of ions on the coagulation and removal of fullerene in aqueous phase, *Sci. Total Environ.*, 2014, **466–467**, 604–608.
25 A. Baun, S. N. Sørensen, R. F. Rasmussen, N. B. Hartmann and C. B. Koch, Toxicity and bioaccumulation of xenobiotic organic compounds in the presence of aqueous suspensions of aggregates of nano-C60, *Aquat. Toxicol.*, 2008, **86**(3), 379–387.
26 R. Floris, K. Nijmeijer and E. R. Cornelissen, Removal of aqueous nC60 fullerene from water by low pressure membrane filtration, *Water Res.*, 2016, **91**, 115–125, available from: http://www.sciencedirect.com/science/article/pii/S0043135415302797.
27 C. Henry and J. A. Brant, Mechanistic analysis of microfiltration membrane fouling by buckminsterfullerene (C60) nanoparticles, *J. Membr. Sci.*, 2012, **415–416**, 546–557.
28 M. Sillanpää, *Natural Organic Matter in Water*, Elsevier, 2015, pp. 1–15.
29 K. L. Chen, B. A. Smith, W. P. Ball and D. H. Fairbrother, Assessing the colloidal properties of engineered nanoparticles in water: case studies from fullerene C60 nanoparticles and carbon nanotubes, *Environ. Chem.*, 2010, **7**(1), 10–27.
30 H. Huang, N. Lee, T. Young, A. Gary, J. C. Lozier and J. G. Jacangelo, Natural organic matter fouling of low-pressure, hollow-fiber membranes: Effects of NOM source and hydrodynamic conditions, *Water Res.*, 2007, **41**(17), 3823–3832.
31 S. Hong and M. Elimelech, Chemical and physical aspects of natural organic matter (NOM) fouling of nanofiltration membranes, *J. Membr. Sci.*, 1997, **132**, 159–181.
32 Q. Li and M. Elimelech, Synergistic effects in combined fouling of a loose nanofiltration membrane by colloidal materials and natural organic matter, *J. Membr. Sci.*, 2006, **278**, 72–82.
33 R. Grillo, A. H. Rosa and L. F. Fraceto, Engineered nanoparticles and organic matter : A review of the state-of-the-art, *Chemosphere*, 2015, **119**, 608–619.
34 W. Zhang, U.-S. Rattanaudompol, H. Li and D. Bouchard, Effects of humic and fulvic acids on aggregation of aqu/nC60 nanoparticles, *Water Res.*, 2013, **47**(5), 1793–1802.
35 A. Philippe and G. E. Schaumann, Interactions of Dissolved Organic Matter with Natural and Engineered Inorganic Colloids: A Review, *Environ. Sci. Technol.*, 2014, **48**, 8946–8962.
36 H. Mashayekhi, S. Ghosh, P. Du and B. Xing, Effect of natural organic matter on aggregation behavior of C60 fullerene in water, *J. Colloid Interface Sci.*, 2012, **374**(1), 111–117.
37 M. Shen, Y. Yin, A. Booth and J. Liu, Effects of molecular weight-dependent physicochemical heterogeneity of natural organic matter on the aggregation of fullerene nanoparticles in mono- and di-valent electrolyte solutions, *Water Res.*, 2014, **71**, 11–20.
38 L. Zhang, Y. Zhang, X. Lin, K. Yang and D. Lin, The role of humic acid in stabilizing fullerene C60 suspensions, *J. Zhejiang Univ., Sci., A*, 2014, **15**(8), 634–642.
39 S. Chae, T. Noeiaghaei, H. Jang, S. Sahebi, D. Jassby and H. Shon, *et al.* Effects of natural organic matter on separation of the hydroxylated fullerene nanoparticles by cross-flow ultrafiltration membranes from water, *Sep. Purif. Technol.*, 2015, **140**, 61–68.
40 J. Duan and J. Gregory, Coagulation by hydrolysing metal salts, *Adv. Colloid Interface Sci.*, 2003, **102**(SUPPL), 475–502.
41 K. L. Chen and M. Elimelech, Influence of humic acid on the aggregation kinetics of fullerene (C60) nanoparticles in monovalent and divalent electrolyte solutions, *J. Colloid Interface Sci.*, 2007, **309**, 126–134.
42 N. Lee, G. Amy, J.-P. Croué and H. Buisson, Identification and understanding of fouling in low-pressure membrane (MF/UF) filtration by natural organic matter (NOM), *Water Res.*, 2004, **38**(20), 4511–4523.
43 L. Fan, J. L. Harris, F. A. Roddick and N. A. Booker, Influence of the characteristics of natural organic matter on the fouling of microfiltration membranes, *Water Res.*, 2001, **35**(18), 4455–4463.
44 T. Carroll, S. King, S. R. Gray, B. A. Bolto and N. A. Booker, The fouling of microfiltration membranes by NOM after coagulation treatment, *Water Res.*, 2000, **34**(11), 2861–2868.
45 K. Kimura, K. Tanaka and Y. Watanabe, Microfiltration of different surface waters with/without coagulation: Clear correlations between membrane fouling and hydrophilic biopolymers, *Water Res.*, 2014, **49**, 434–443, available from: http://dx.doi.org/10.1016/j.watres.2013.10.030.
46 R. Shang, F. Vuong, J. Hu, S. Li, A. J. B. Kemperman and K. Nijmeijer, *et al.* Hydraulically irreversible fouling on ceramic MF/UF membranes: Comparison of fouling indices, foulant composition and irreversible pore narrowing, *Sep. Purif. Technol.*, 2015, **147**, 303–310, available from: http://dx.doi.org/10.1016/j.seppur.2015.04.039.
47 H. Yamamura, K. Kimura and Y. Watanabe, Mechanism Involved in the Evolution of Physically Irreversible Fouling in Microfiltration and Ultrafiltration Membranes Used for Drinking Water Treatment, *Environ. Sci. Technol.*, 2007, **41**(19), 6789–6794.
48 A. I. Schafer, Microfiltration of colloids and natural organic matter, *J. Membr. Sci.*, 2000, **171**, 151–172.
49 E. R. Cornelissen, D. Chasseriaud, W. G. Siegers, E. F. Beerendonk and D. Van Der Kooij, Effect of anionic fluidized ion exchange (FIX) pre-treatment on nanofiltration (NF) membrane fouling, *Water Res.*, 2010, **44**(10), 3283–3293.
50 Y. K. Jung, M. J. Kim, Y.-J. Kim and J. Y. Kim, Limitation of UV-Vis absorption analysis for determination of aqueous colloidal fullerene (nC60) at high ionic strength, *KSCE J. Civ. Eng.*, 2013, **17**(1), 51–59.
51 A. Kolkman, E. Emke, P. S. Bäuerlein, A. Carboni, D. T. Tran and T. L. ter Laak, *et al.* Analysis of (functionalized) fullerenes in water samples by liquid chromatography coupled to high-resolution mass spectrometry, *Anal. Chem.*, 2013, **85**(12), 5867–5874.

52 K. L. Chen and M. Elimelech, Relating colloidal stability of fullerene (C60) nanoparticles to nanoparticle charge and electrokinetic properties, *Environ. Sci. Technol.*, 2009, **43**(19), 7270–7276.
53 J. Brant, H. Lecoanet, M. Hotze and M. Wiesner, Comparison of electrokinetic properties of colloidal fullerenes (nC60) formed using two procedures, *Environ. Sci. Technol.*, 2005, **39**(17), 6343–6351.
54 R. Floris, E. Emke, J. Haftka, B. Hofs, K. Nijmeijer and E. R. Cornelissen, Removal efficiency of nC60 nanoparticles by microfiltration membranes, in *IWA Symposium on Environmental Nanotechnology*, Nanjing, 2013, pp. 245–246.
55 K. W. Trzaskus, W. M. de Vos, A. Kemperman and K. Nijmeijer, Towards controlled fouling and rejection in dead-end microfiltration of nanoparticles - Role of electrostatic interactions, *J. Membr. Sci.*, 2015, **496**, 174–184.
56 X. Shi, G. Tal, N. P. Hankins and V. Gitis, Fouling and cleaning of ultrafiltration membranes: A review, *J. Water Process Eng.*, 2014, **1**, 121–138.
57 S. Chellam and W. Xu, Blocking laws analysis of dead-end constant flux microfiltration of compressible cakes, *J. Colloid Interface Sci.*, 2006, **301**, 248–257.
58 S. Chellam and N. G. Cogan, Colloidal and bacterial fouling during constant flux microfiltration: Comparison of classical blocking laws with a unified model combining pore blocking and EPS secretion, *J. Membr. Sci.*, 2011, **382**(1–2), 148–157.
59 E. M. Hotze, T. Phenrat and G. V. Lowry, Nanoparticle Aggregation: Challenges to Understanding Transport and Reactivity in the Environment, *J. Environ. Qual.*, 2010, **39**(6), 1909.
60 H. Hyung and J.-H. Kim, Dispersion of C(60) in natural water and removal by conventional drinking water treatment processes, *Water Res.*, 2009, **43**(9), 2463–2470.
61 D. Lin, N. Liu, K. Yang, B. Xing and F. Wu, Different stabilities of multiwalled carbon nanotubes in fresh surface water samples, *Environ. Pollut.*, 2010, **158**(5), 1270–1274.
62 P. Nguyen and E. Asmatulu, *Nanotechnology Safety*, Elsevier, 2013, pp. 57–72.
63 D. Jermann, W. Pronk and M. Boller, Mutual Influences between Natural Organic Matter and Inorganic Particles and Their Combined Effect on Ultrafiltration Membrane Fouling, *Environ. Sci. Technol.*, 2008, 9129–9136.
64 W. Yuan, A. Kocic and A. L. Zydney, Analysis of humic acid fouling during microfiltration using a pore blockage–cake filtration model, *J. Membr. Sci.*, 2002, **198**(1), 51–62.
65 A. G. Fane, W. Xi and W. Rong, Interface Science in Drinking Water Treatment - Theory and Application, *Interface Science and Technology*, Elsevier, 2006, vol. 10.
66 S. Li, S. G. J. Heijman, J. Q. J. C. Verberk, P. Le, J. Lu and A. J. B. Kemperman, *et al.* Fouling control mechanisms of demineralized water backwash: Reduction of charge screening and calcium bridging effects, *Water Res.*, 2011, **5**(0), 0–11.
67 Astaraee R. Seifollahy, T. Mohammadi and N. Kasiri, Analysis of BSA, dextran and humic acid fouling during microfiltration, experimental and modeling, *Food Bioprod. Process.*, 2015, **94**, 331–341.
68 J. Mendret, C. Guigui, P. Schmitz and C. Cabassud, In situ dynamic characterisation of fouling under different pressure conditions during dead-end filtration: Compressibility properties of particle cakes, *J. Membr. Sci.*, 2009, **333**, 20–29.